AD712505

NAVAL AIR DEVELOPMENT CENTER

Johnsville, Warminster, Pennsylvania

NADC-MR-7017 16 September 1970

Heat Transfer Through Fabrics

Naval Air Systems Command
AirTask A34531/202/70F32523401
Work Unit No. 2

AirTask A34531/202/70F12524402
Work Unit No. 7

THIS REPORT HAS BEEN APPROVED FOR PUBLIC RELEASE AND SALE; ITS DISTRIBUTION IS UNLIMITED

OCT 12 1970

41

DEPARTMENT OF THE NAVY
NAVAL AIR DEVELOPMENT CENTER
JOHNSVILLE
WARMINSTER, PA. 18974

Aerospace Medical Research Department

NADC-MR-7017 16 September 1970

Heat Transfer through Fabrics[1]

Naval Air Systems Command
AirTask A34531/202/70F32523401
Work Unit No. 2

AirTask A34531/202/70F12524402
Work Unit No. 7

THIS REPORT HAS BEEN APPROVED FOR PUBLIC RELEASE AND SALE; ITS DISTRIBUTION IS UNLIMITED

Prepared by: Alice M. Stoll
Maria A. Chianta

Approved by: Harald J. von Beckh, M.D.
Research Director
Aerospace Medical Research Department

Released by: D. Morris, CAPT, MC, USN
Director
Aerospace Medical Research Department

---

[1]Presented in part at the USAF Air Force Materials Laboratory Symposium, Miami Beach, Florida, May 1970.

SUMMARY

Heat is transferred through fabrics by convection, conduction and radiation and under certain circumstances by vaporization. Each mode is subject to different physical principles but the effect of the total heat absorbed by underlying skin is the same: if the resultant skin temperature rise is sufficiently high and maintained sufficiently long, injury results. The extent of injury is predicted under certain controlled conditions and these conditions may be used to disclose protection principles appropriate to each mode of transfer.

TABLE OF CONTENTS

	Page
SUMMARY	ii
INTRODUCTION	1
BACKGROUND	1
HEAT TRANSFER BY CONVECTION AND CONDUCTION	4
HEAT TRANSFER BY RADIATION	13
VAPORIZATION	17
PHYSIOLOGICAL PROTECTION	17
ASSESSMENT OF PROTECTIVE CAPACITY	24
REFERENCES	33

LIST OF FIGURES

Figure	Title	Page
1	Heating and cooling of skin by thermal irradiation	2
2	Tissue damage rate change with temperature increase	3
3	Tissue damage integral indicative of the blister endpoint	5
4	Summary of basic features of the burn injury mechanism	6
5	Graphic representation of increased heat transfer as receiver orientation to flames approaches the perpendicular	8
6	Temperature rise per unit heat flux at surface, interface and depth within layer 2 (simulated skin) and comparison of experimental and theoretical data	11
7	Decrease in temperature rise in skin simulant behind double-layer fabric as air space between layers increases to an optimum corroborated by increase in exposure time to produce white burn in skin of anaesthetized rat	12

LIST OF FIGURES

(Continued)

Figure	Title	Page
8	Comparison of spectral reflectance and transmittance of a green and of a white fabric	14
9	Computation of energy transmitted	15
10	Comparison of strength-duration curves for white burns produced by flame contact and by thermal radiation	18
11	Human skin tolerance time to absorbed thermal energy delivered in a rectangular heat pulse	19
12	Human skin tolerance time indicated by the temperature rise measured in a skin simulant at 3 seconds' exposure to a rectangular heat pulse	21
13	Minimal thickness of insulation required to limit temperature rise at various exposure times	22
14	Maximum skin surface temperature during exposure productive of a blister endpoint at fixed heat absorption rates	25
15	Distribution of temperature measurement sites and weighting of areas with respect to total surface	26
16	Fuel flame facility for exposures in full-scale protection evaluations	29
17	Quartz lamp heat source with F4 fuselage backed out from under arc	31

LIST OF TABLES

Table	Title	Page
1	Correlation of Heat Absorption, Temperature Rise and Insulation Thickness	23

Introduction

Our interest in heat transfer through fabrics is centered on the production and prevention of injury to the skin of a human who might wear the fabrics in clothing. Our understanding of the burn mechanism (1) is not perfect or complete but it is sufficient for the practical purposes concerned here.

Background

Figure 1 shows the temperature rise in skin subjected to radiation sufficient to cause a blister in about 34 seconds and in about 6 seconds. The lower limit of injurious temperatures is about 44°C. This temperature refers to the basal layer of skin, about 80μ below the surface, where the base of the blister forms. The surface temperature is, of course, higher and where the incident radiation is greater, the difference between surface and depth temperatures is greater. Equivalent damage is produced at different peak temperatures, about 52° for the lower intensity and 58° for the higher. Injury goes on any time and all the time that the skin temperature remains above 44°C. This means that injury continues during cooling as well as heating. The rate at which the injury proceeds is shown in Figure 2. It increases logarithmically with linear increase in temperature. Thus, damage occurs a hundred times faster at 50°C than at 45°. Extrapolation of the data indicates that at a tissue temperature of about 72°C the skin is destroyed

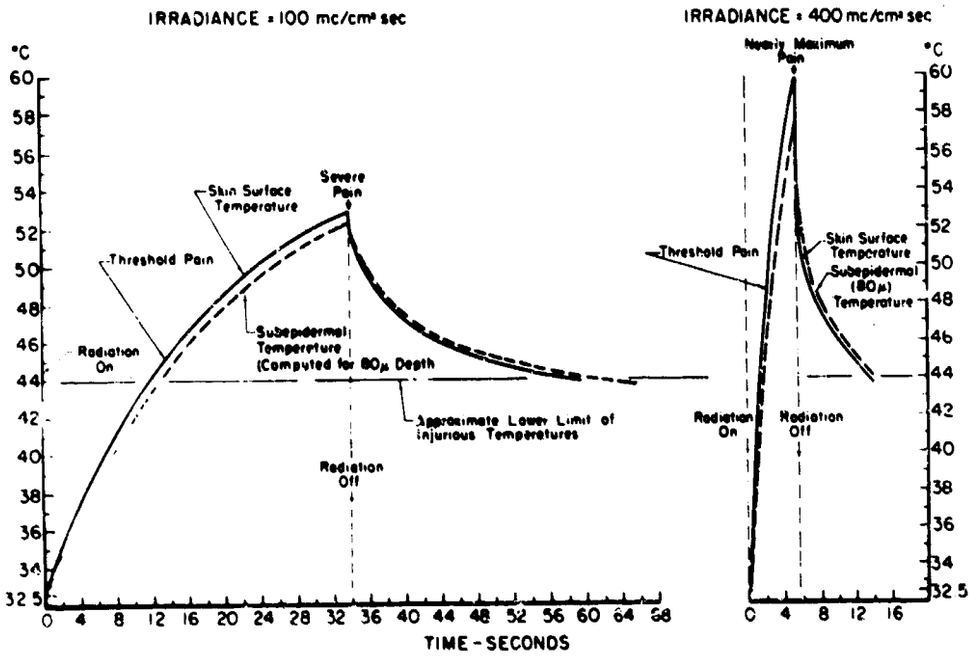

Figure 1. Heating and cooling of skin by thermal irradiation.

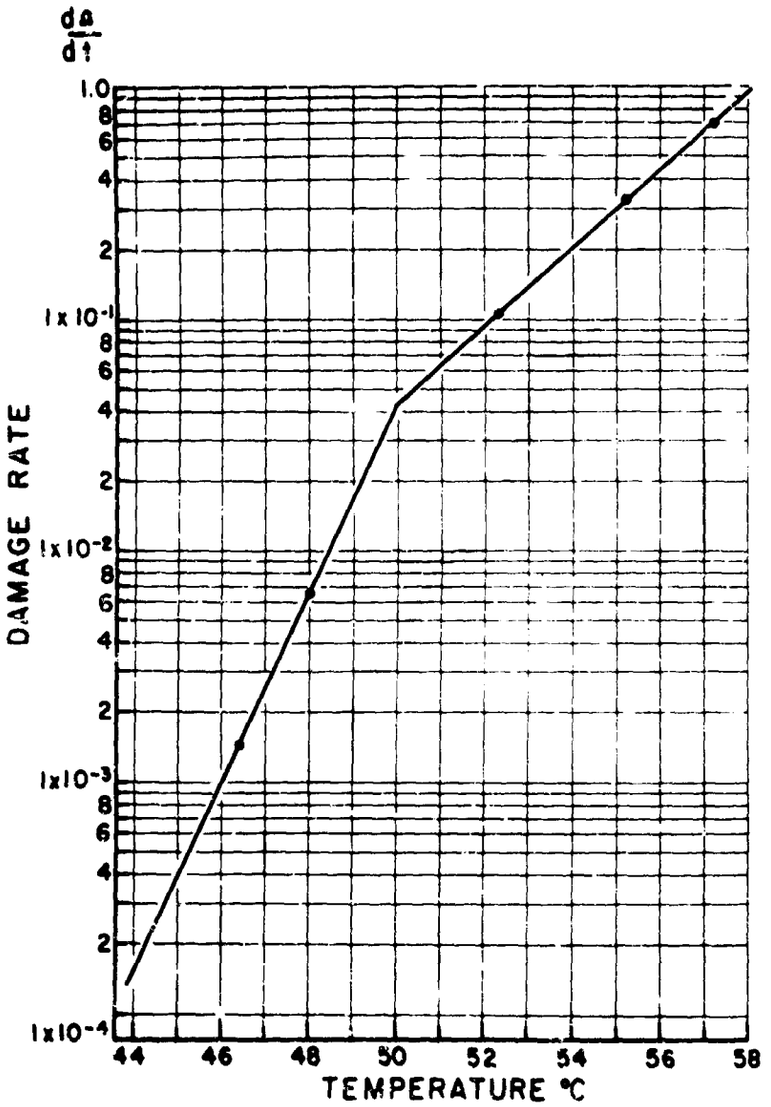

Figure 2. Tissue damage rate change with temperature increase.

virtually instantaneously. Figure 3 shows the computation of total injury at the two levels of irradiation shown in Figure 1. Here we see the damage rate plotted against the time at which the corresponding temperature occurred. Then by means of integration of this curve during heating and during cooling, total damage is obtained (2,3). A total of 1.0 indicates a blister end point, i.e., a blister forming within 24 hours of the irradiation. With the lower intensity radiation, 90% of the total damage occurs during heating, whereas with the higher intensity, 65% occurs during heating and 35% during cooling (1). This accounts for the well-known prevention of a blister by prompt application of ice to an exposed area. If done soon enough a third of the injury can be eliminated.

These basic facts concerning the burn mechanism, which are vital in assessing the physiological effects of heat transfer through fabrics, are consolidated in Figure 4: A. Skin temperature rises on absorption of heat; damage occurs at 44°C, increases rapidly at higher temperatures and persists as long as the temperature remains above 44°; B. The damage rate increases logarithmically with linear increase in tissue temperature; C. When the temporal integral of damage rate equals unity the blister end point is attained, less than unity indicates reversible damage and greater than unity more severe damage than blistering: and finally, D. As the rate of heat absorption by the skin increases, a greater percentage of the total damage occurs during cooling, after removal of the heat source, and may amount to as much as 35%.

Heat Transfer by Convection and Conduction

In burn accidents, the commonest source of injury is flame contact.

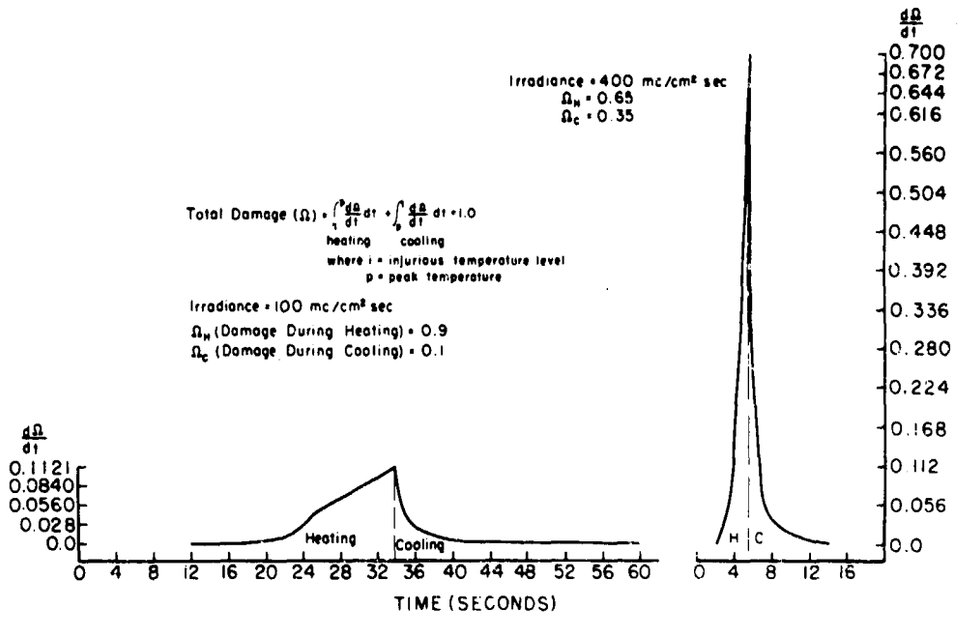

Figure 3. Tissue damage integral indicative of the blister endpoint.

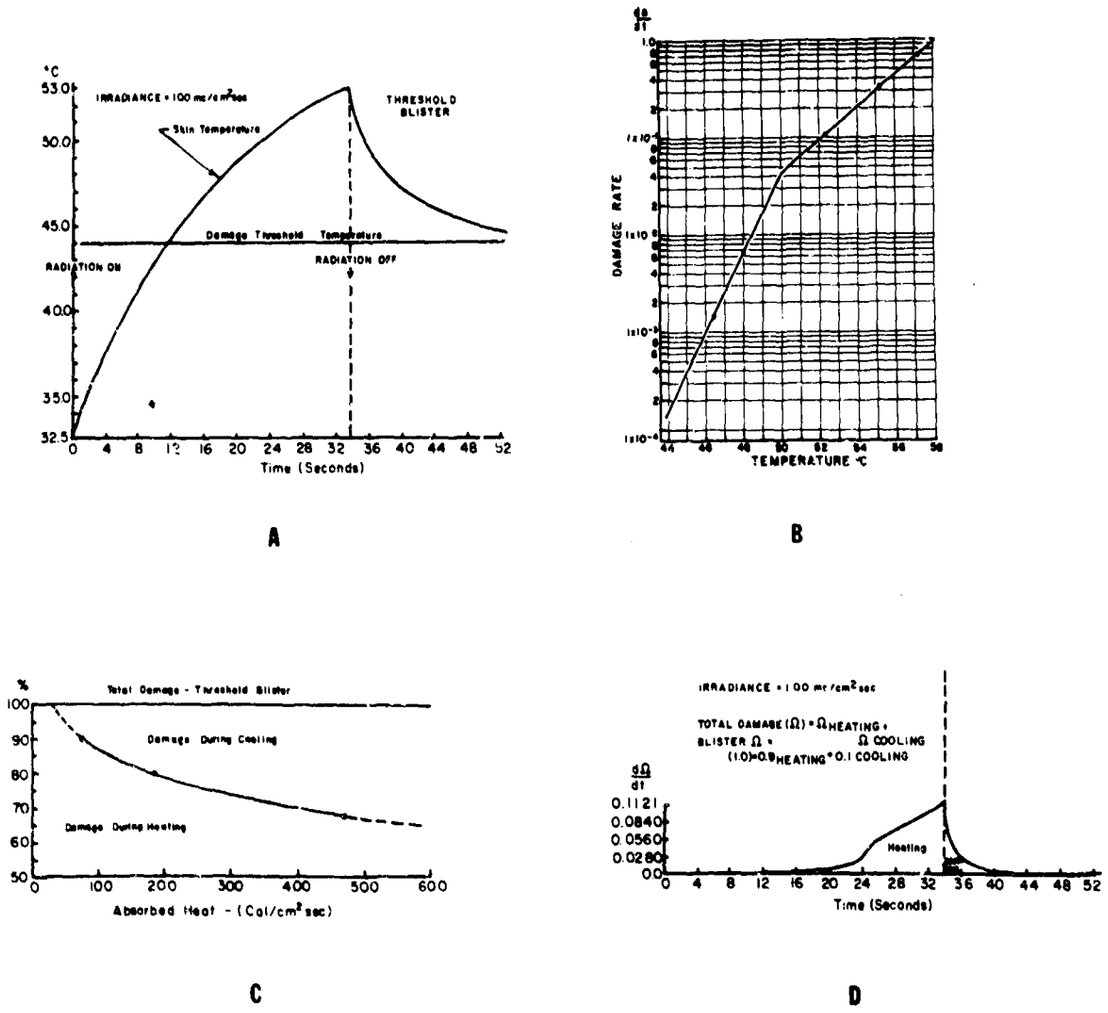

Figure 4. Summary of basic features of the burn injury mechanism.

Here we are concerned with two processes, convection and conduction. Figure 5 depicts, simply, degrees of heat transferred from the same source depending on the orientation of the receiver, in this instance, assumed to be a section of fabric-covered skin exposed to flames from a Meker burner. In the first section the receiver is oriented parallel to the flames so that with respect to the basal layer of the skin, relatively little heat is transferred since the gas flow force is upwards. The surface of the fabric is heated by convection primarily with some hot gas conduction contribution. Beyond the fabric surface heating occurs by conduction, penetrating as a function of the thermal properties of the fabric and the skin to and beyond the basal layer. The graph depicts schematically the temperature rise at surface, fabric-skin interface and at depth in the underlying layer. The next two sections suggest how the heat transferred increases as the receiver is oriented more perpendicular to the flames until the maximum is reached at the 90° angle. Again, the graphs indicate the increase in the various temperature rises under these circumstances. Equations derived by Griffith and Horton (4) provide precise measurements of the temperatures involved if the physical and thermal characteristics of both layers are known. As shown in Equation 1, as corrected in Stoll (5):

<u>Equation 1</u>- TEMPERATURE RISE AT DEPTH IN LAYER 2

$$U_2 = \frac{2H\lambda\sqrt{D_1}}{\gamma}\sum_{n=0}^{n=\infty}\left(-\frac{1}{\gamma}\right)^n \left\{2\sqrt{\frac{D_2 t}{\pi}}\, e^{-\{x-a\{1-\sqrt{D_2/D_1}\,(2n+1)\}\}^2/4D_2 t} - [x-a\{1-\sqrt{D_2/D_1}\,(2n+1)\}]\left(1-\mathrm{erf}\,\frac{x-a\{1-\sqrt{D_2/D_1}\,(2n+1)\}}{2\sqrt{D_2 t}}\right)\right\}$$

FLAME CONTACT HEATING

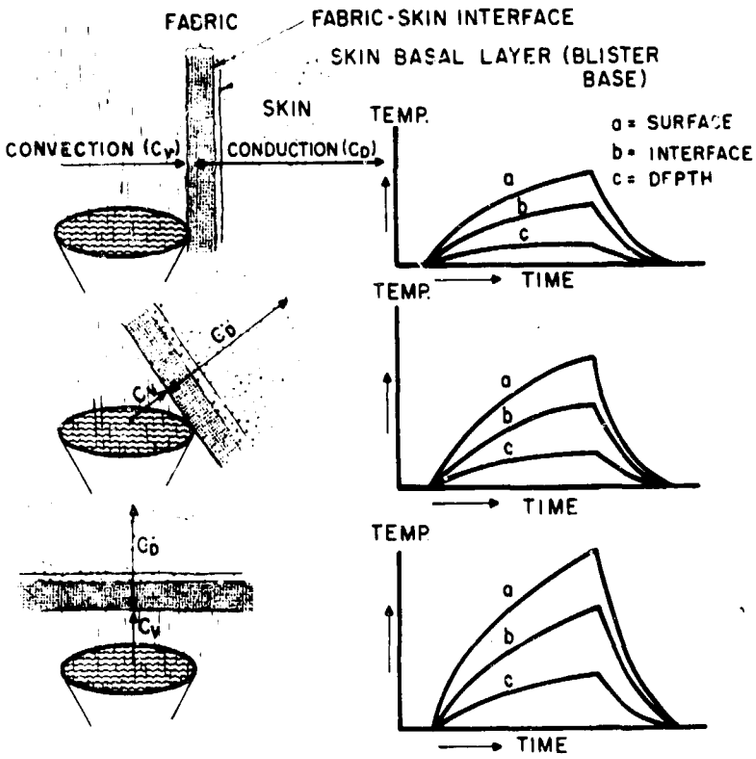

Figure 5. Graphic representation of increased heat transfer as receiver orientation to flames approaches the perpendicular.

where

subscript 1 refers to top layer 1, subscript 2 refers to base layer 2

and U = Temperature rise

H = Heat flux perpendicular to surface

X = Total thickness from surface to point of temperature rise measurement

a = Thickness of layer 1

D = Thermal diffusivity = k/S

k = Thermal conductivity

S = Volume specific heat (density x specific heat)

$$\gamma = \frac{k_2 S_2 + \sqrt{k_1 S_1 k_2 S_2}}{k_2 S_2 - \sqrt{k_1 S_1 k_2 S_2}}$$

$$\lambda = (k_2\sqrt{D_1} - k_1\sqrt{D_2})^{-1}$$

the temperature at depth, U_2, may be found if the heat flux at the surface, as well as the properties of both layers, is known. Conversely, if the temperature at depth is measured the equation may be solved for heat flux. If the temperature at depth, the heat flux, and the properties of one layer are known, then the equation may be rearranged to solve for the diffusivity of the other layer. From additional equations, 2 and 3, the temperature rise at the surface and the interface can also

Equation 2 - TEMPERATURE RISE AT SURFACE

$$U_0 = \frac{H}{k_1}\left[2\sqrt{\frac{D_1 t}{\pi}} - \frac{4}{\gamma}\sum_{n=0}^{n=\infty}\left(-\frac{1}{\gamma}\right)^n \left\{\sqrt{\frac{D_1 t}{\pi}}\, e^{-a^2\frac{(n+1)^2}{tD_1}} - a(n+1)\left(1 - \operatorname{erf}\frac{a(n+1)}{\sqrt{D_1 t}}\right)\right\}\right]$$

Equation 3 - TEMPERATURE RISE AT INTERFACE

$$U_3 = \frac{H}{k_1}\sum_{n=0}^{n=\infty}\left(-\frac{1}{\gamma}\right)^n\left(1-\frac{1}{\gamma}\right)\left[2\sqrt{\frac{D_1 t}{\pi}}\, e^{-\left(\frac{a(2n+1)}{2\sqrt{D_1 t}}\right)^2} - a(2n+1)\left(1 - \operatorname{erf}\frac{a(2n+1)}{2\sqrt{D_1 t}}\right)\right]$$

be found. We have validated these equations experimentally (5) in two-layer assemblies of silicone rubber and skin simulant materials of precisely known properties. The agreement between the experimental and the theoretical data is excellent as shown in Figure 6. The same equations and procedures are directly applicable to fabric-skin simulant assemblies and have been used to determine properties such as thermal conductivity and diffusivity. We will see later how they may be used also to determine the minimal thickness of insulation required to limit temperature rise to a fixed value in the underlying layer when it is in firm contact with the outer layer.

One of the most important aspects of convective transfer limitation is the incorporation of air spaces between layers. As seen in Figure 7 the temperature rise behind a double layer of fabric separated by an air space is less than that behind the same assembly without an air space. This effect increases to an optimal width and thereafter diminishes as convection currents arise between the layers and cause the outer one to perforate. These results were corroborated in living skin of anaesthetized, depilated white rats covered by the same assemblies and exposed to the same flame source. It is seen that the exposure time to produce a white burn increased with air space width to the same point as in the inert assembly. Thereafter, the outer layer perforated as before and the exposure time diminished. The fact that exposure time was almost tripled by insertion of a 4 mm air space is dramatic evidence of the effectiveness of such spacing.

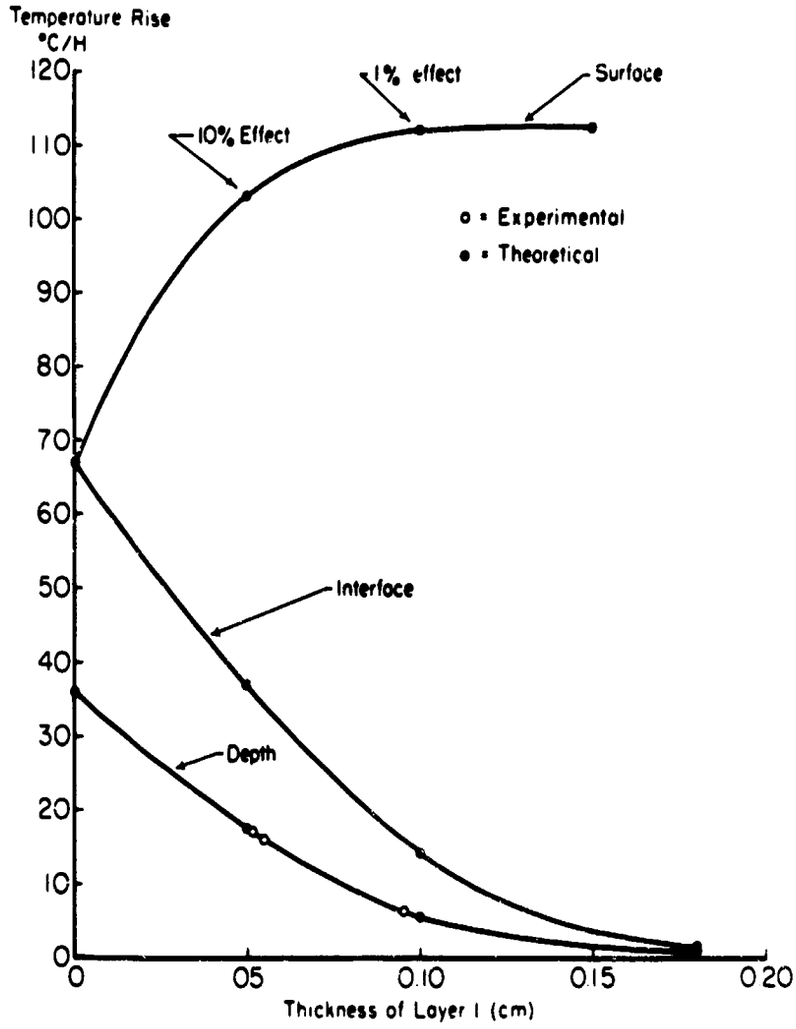

Figure 6. Temperature rise per unit heat flux at surface, interface and depth within layer 2 (simulated skin) and comparison of experimental and theoretical data.

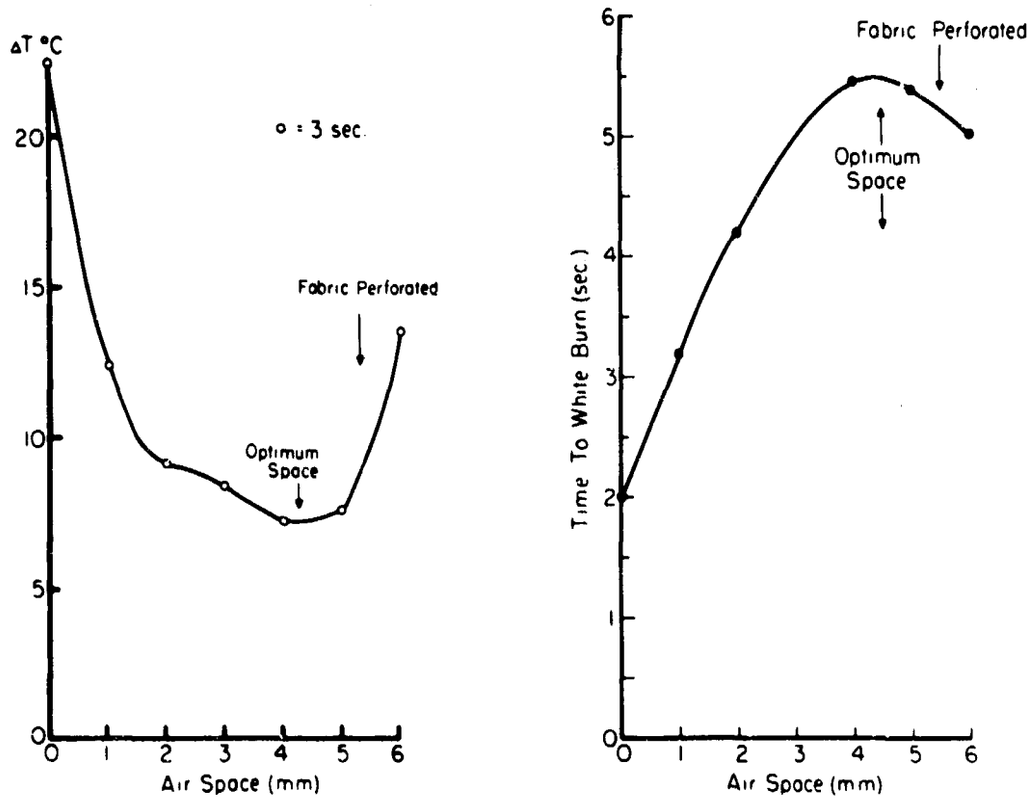

Figure 7. Decrease in temperature rise in skin simulant behind double-layer fabric as air space between layers increases to an optimum corroborated by increase in exposure time to produce white burn in skin of anaesthetized rat.

Heat Transfer by Radiation

The most complicated mode of heat transfer in the fabric-skin system is radiation because the optical properties of both fabric and skin markedly affect the heat absorption characteristics of the system. Of course, total reflection of incident radiation prevents any heat transfer through the fabric and this effect can be accomplished to a very large degree by highly polished surfaces. However, such surfaces are usually impractical in clothing items except for very special cases like fire-fighters suits intended for short-term wear, or the complex, temperature-controlled systems for space travel. Ordinary long-term use is best served by relatively dark colors and light-weight fabrics. To arrive at acceptable materials within these requirements it is necessary to establish the spectral characteristics of the radiation concerned in conjunction with the optical and thermal properties of other materials under consideration. Many fabrics of fairly dark color are 60-70% reflective at wavelengths in the near infra-red (e.g., Figure 8). Almost all fabrics irrespective of color reflect poorly in the far infra-red and the ultraviolet, while light colors and white reflect well in the visible range. Transmittance is also crucial since any energy transmitted through the fabric affects the skin just as though there were no cover on it at all. Figure 9 illustrates the method for determining approximately how much energy will be absorbed by any given system. First it is necessary to know the spectral distribution of the source energy - in this instance, a black body at 2600°K - then, the spectral reflectance and transmittance of the fabric. Only transmittance

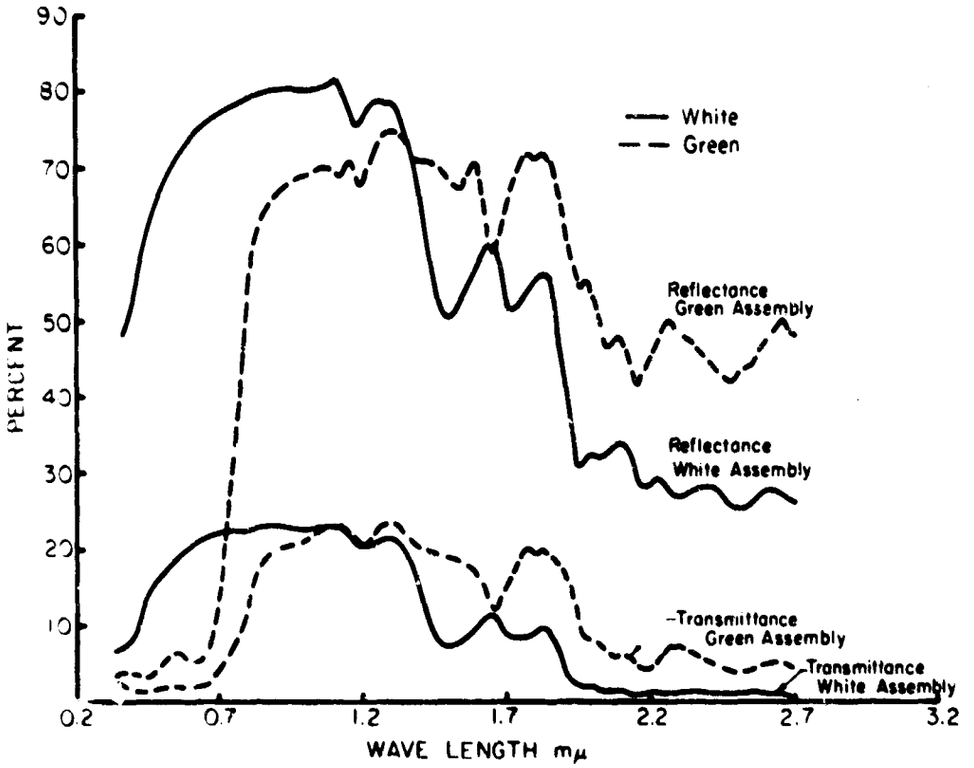

Figure 8. Comparison of spectral reflectance and transmittance of a green and of a white fabric.

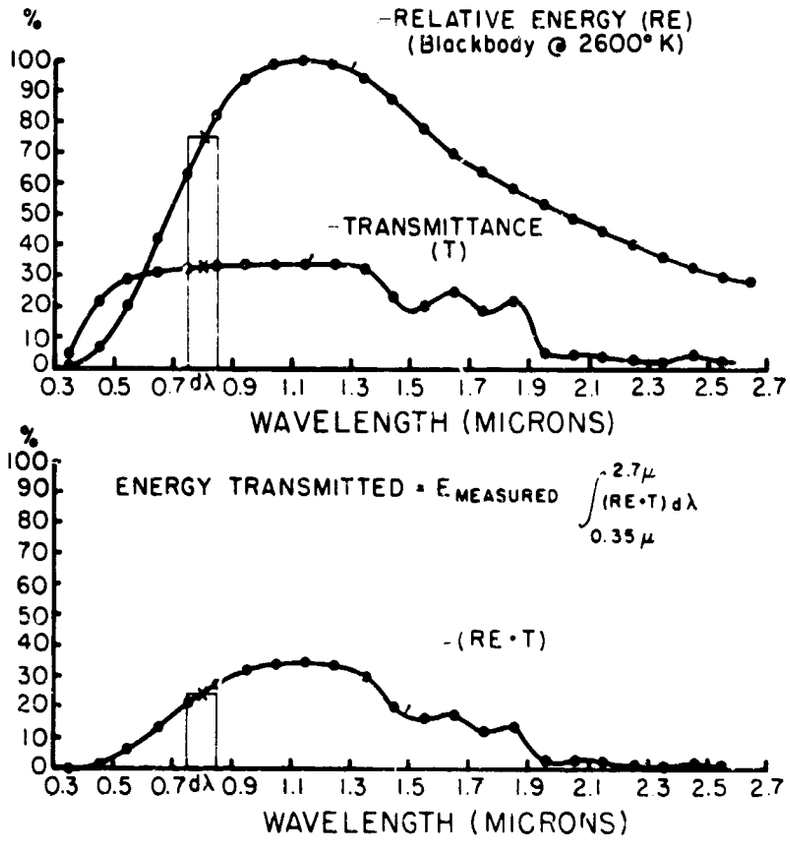

Figure 9. Computation of energy transmitted.

is represented here but reflectance is handled exactly the same way. The percentage at each wavelength is multiplied by the percentage of maximum energy present in the spectrum at that wavelength. This product is then plotted against wavelength at each point in the spectral range. Integration may be carried out either numerically as the sum of the energy in each wavelength interval or graphically as the area under the derived curve. Either way, the integral for reflectance and for transmittance is found. Then an independent measurement of total radiation is made with a suitable radiometer and this energy multiplied by the reflectance integral gives the energy reflected and, similarly, multiplied by the transmittance integral gives the energy transmitted directly to the underlying surface. The total energy measured minus reflected and transmitted energy is the absorbed fraction. Where the underlying surface itself reflects certain wavelengths, further considerations are required to assess this effect. It is usually simpler to measure the total temperature rise, compute the fraction due to absorbed energy conducted to the surface and find the remainder which is due to the transmitted energy. However, for the purpose of selecting suitable fabrics it is often sufficient to compare only the reflection and transmission data of the fabrics themselves to predict their behavior in thermal protection.

Vaporization

A complete treatment of the subject should note that vaporization also may transfer heat through fabrics either indirectly, as in the instance of perspiration absorption and evaporation, or directly by transpiration through interstices. This transfer, however, is in the opposite direction from the others under consideration here and while important in long-term, environmental exchange and comfort studies is relatively unimportant in burns.

Physiological Protection

Since our present interest is protection from burns, we pursue the basic concept that burn injury is ultimately related to tissue temperature elevation for a sufficient time. We have shown that regardless of the mode of application of heat, the temperature rise and therefore the tolerance time is related to heat absorbed by the skin (6). Figure 10 shows such data for convection and for radiation burns in anaesthetized rats. When the time to produce a standard white burn is plotted against heat absorption rates the curves are superimposed within experimental limits. This observation permitted the generalization of human burn data obtained in radiation studies to any situation in which heat is absorbed by the skin at a constant rate in a square-wave pattern (7). Figure 11 shows these data plotted on log-log coordinates of tolerance time and energy absorption rate. The shortest time line represents pain threshold; the longest is the time to blistering. A line drawn midway between these two and labelled "Survival" represents the parameter where pain is felt but the skin damage is reversible, without blistering. The data obtained on rats are shown also and these all lie

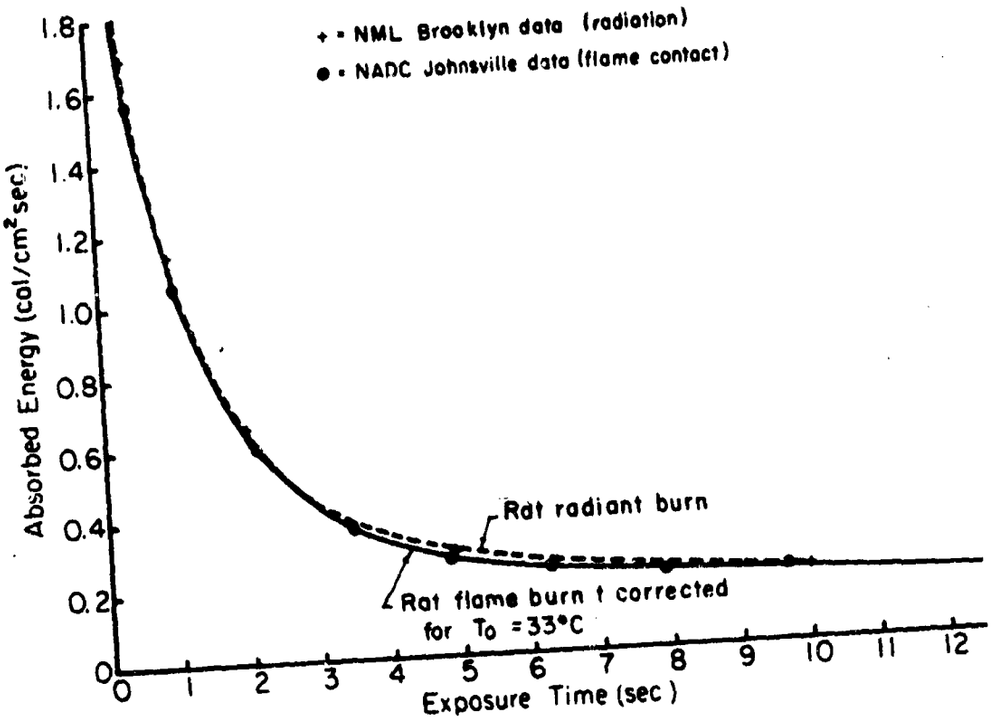

Figure 10. Comparison of strength-duration curves for white burns produced by flame contact and by thermal radiation.

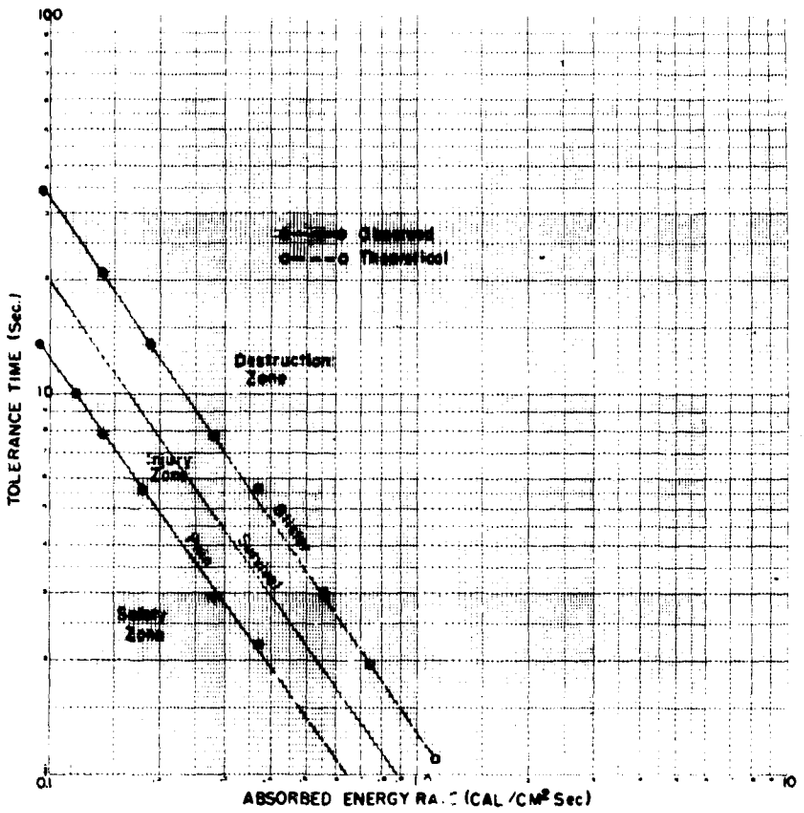

Figure 11. Human skin tolerance time to absorbed thermal energy delivered in a rectangular heat pulse.

within the area between pain and blister. At the lower end of the tolerance time, where experimental data in the human is derived from theory, the rat observations skew towards longer exposure times. Therefore, any error in this area leans toward the side of safety.

For convenience these data have been transposed to temperature rise in a skin simulant measured at 3 seconds' exposure time as shown in Figure 12. This type of measurement yields the same information as shown in the previous slide, quickly and easily, under controlled experimental conditions in the laboratory. By means of additional charts computed by Griffith and Horton's equations and exemplified in Figure 13, the minimal thickness of insulation, of a material of given thermal properties, required to limit temperature rise can also be determined. For instance, in Figure 13 it is seen that for a particular fabric on the skin simulant at 3-seconds' exposure a thickness of about 3 mm is required to limit the temperature rise to 20°C at an absorption rate of one calorie/cm^2sec. As the time increases, the thickness also increases so that a family of curves is generated. Table I shows how the energy absorption rate, temperature rises and insulation thickness vary as the exposure time increases. Where blistering is the end point, as the exposure time increases from 3 seconds to 6 seconds the permissible absorption rate drops from 0.55 to 0.335; the temperature rise in the skin simulant drops from 20.0 to 12.3; the maximum skin temperature drops from 61.2 to 58.1 and the insulation thickness more than doubles.

If one wishes to limit injury to the survival parameter, the same data may be derived by referring to the tolerance chart and working back. Thus,

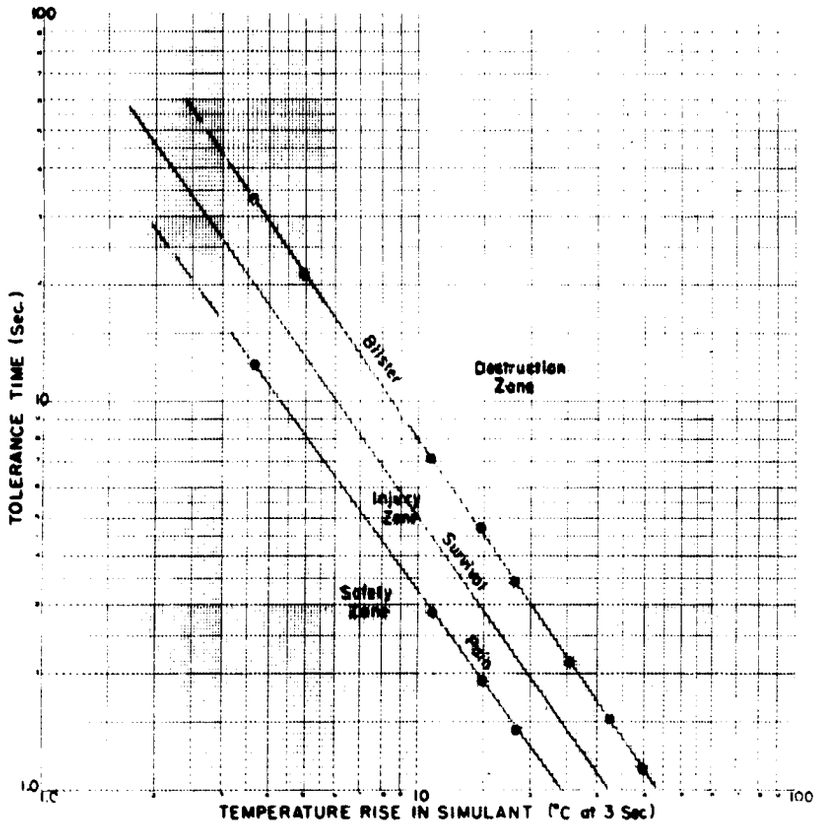

Figure 12. Human skin tolerance time indicated by the temperature rise measured in a skin simulant at 3 seconds' exposure to a rectangular heat pulse.

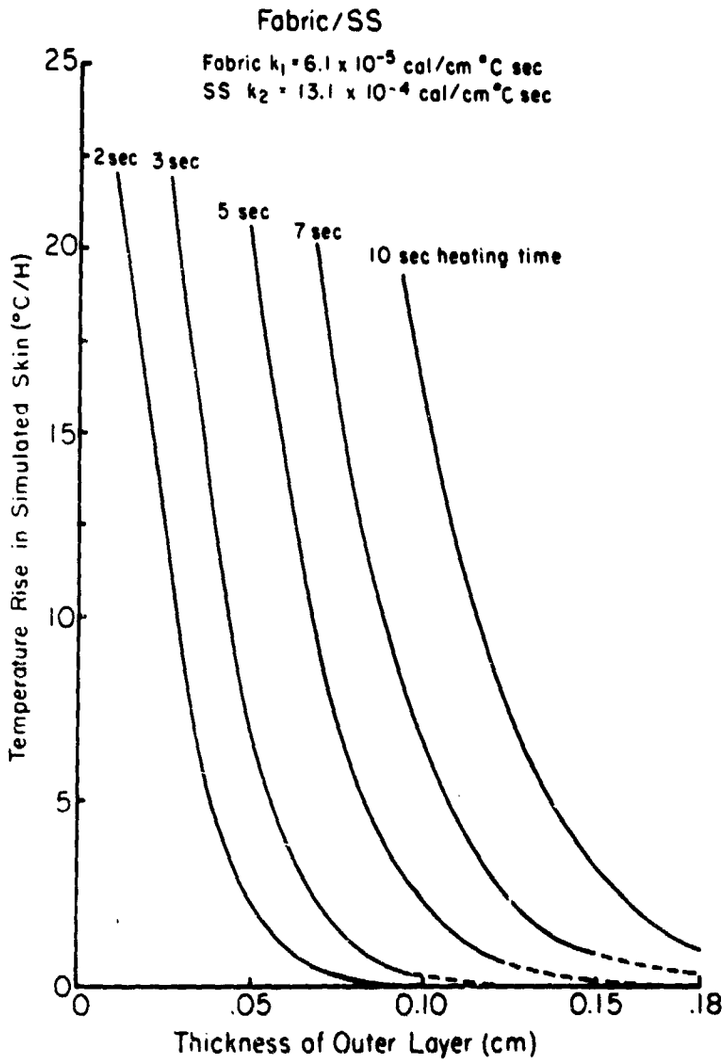

Figure 13. Minimal thickness of insulation required to limit temperature rise at various exposure times.

Blister Parameter

Exposure Time (sec)	Energy Absorption (cal/cm^2 sec)	ΔT_{ss} @ 3 sec (°C)	Max. T_s (°C)	Insulation* (mm)
3	0.550	20.0	61.2	0.28
6	0.335	12.3	58.1	0.72
10	0.235	8.5	55.9	1.22

"Survival" Parameter

Exposure Time (sec)	ΔT_{ss} @ 3 sec (°C)	Energy Abs. $\left(\frac{\Delta T_{ss}}{36.2}\right)$ (cal/cm^2 sec)	Max. T_s (°C)	Insulation* (mm)
3	14.5	0.400	59.2	0.36
6	8.9	0.246	56.2	0.80
10	6.0	0.166	54.1	1.31

ΔT_{ss} = Temperature rise at depth in skin simulant.

T_s = Living human skin surface temperature.

* Insulation thicknesses shown refer to a specific material of thermal conductivity 6.1×10^{-5} cal/cm^2 sec and volume specific heat 0.196 cal/cm^2 °C, exposed to 1 cal/cm^2 sec incident energy. Similar data can be generated for any material of known thermal properties.

Table I. Correlation of Heat Absorption, Temperature Rise and Insulation Thickness

at 3 seconds' exposure time the permissible simulant temperature rise is 14.5°; this divided by 36.2°C, the temperature rise at 1 cal/cm^{2}sec, gives the permissible energy absorption, 0.40 cal/cm^{2}sec. Empirical data (Figure 14) show that at this rate the maximum skin surface temperature is 59.2°C, and the insulation read from the appropriate family of curves is 0.36 mm, as compared with 0.28 mm for the blister endpoint.

While these derivations depend upon stringently controlled conditions which do not occur in the real life situation they do represent the "worst case" picture for unignited fabrics and are extremely valuable in assessing the comparative efficacy of different fabrics in terms of physiological protection.

Assessment of Protective Capacity

When small-scale studies indicate feasibility of certain fabrics as thermal protective clothing candidates these materials are made up into prototype garments. The prototypes are subjected to full-scale evaluations of their protective capacity under appropriate experimental conditions. Two specific areas are studies in our work, the first dealing with flame contact and the second, high intensity thermal radiation commensurate with that from thermonuclear detonations. However, as far as the assessment of burn distribution and severity is concerned, the instrumentation and techniques are the same for both modes of heat transfer. Areas on the body surface are selected according to the DuBois percentage presentation (8) shown in Figure 15. The percentage of the total surface represented by each portion of the body is

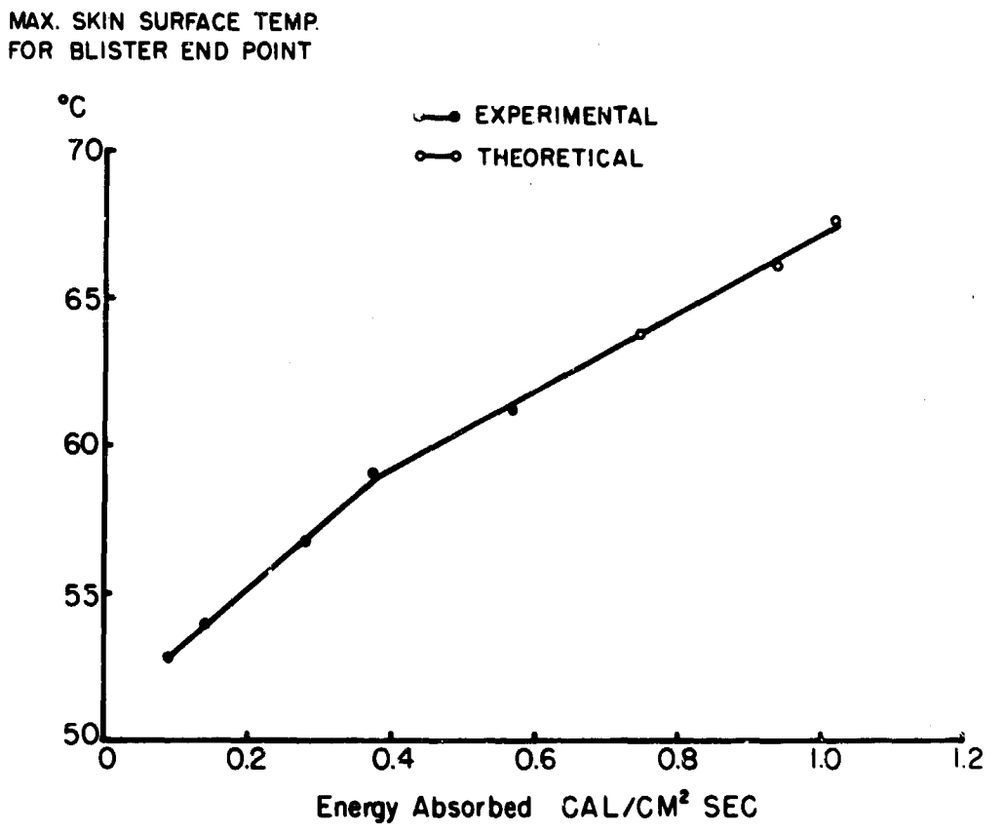

Figure 14. Maximum skin surface temperature during exposure productive of a blister endpoint at fixed heat absorption rates.

DISTRIBUTION OF TEMPERATURE INDICATORS

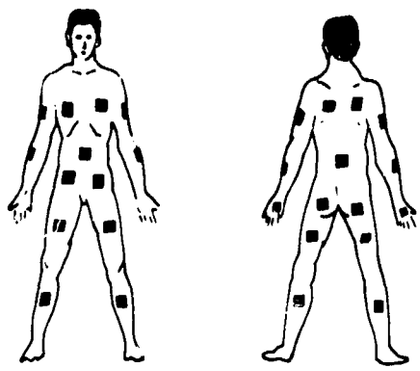

SURFACE AREA WEIGHTING

% OF TOTAL AREA		NUMBER OF SITES IN AREA
HEAD	7	4 (WHEN USED)
TRUNK	35	10
ARMS	14	4
HANDS	5	2 (WHEN USED)
THIGHS	19	4
LEGS	13	4
FEET	7	0 (NOT USED)

Figure 15. Distribution of temperature measurement sites and weighting of areas with respect to total surface.

shown, and the number of sites for measurement of surface temperature rise within each section is indicated. The patches on the body surface (Figure 15) mark these sites; head, feet and sometimes hands are excepted as special cases. A store manikin is completely covered with leather except for the "special case" areas. Leather is used because it is pliable and relatively sturdy and temperature rise proceeds at a rate three times that of living human skin. The latter feature permits the temperature rise measured on the leather surface to be converted to temperature rise in the living skin (9). From the maximum temperature achieved and the exposure time the severity of burns may be predicted by procedures utilizing the data shown in Figure 11. Then by weighting these observations in accordance with the ratios shown in Figure 15, the percentage of body surface affected may be ascertained. For instance, 10 sites on the torso are observed; if 5 of these indicate burns and 5 no burns then the portion of the body affected is $\frac{5}{10}$ x 35% or 17.5% of the total surface; similarly, if 3 out of 4 sites on the arms indicate burns, then $\frac{3}{4}$ x 14% = 10.5% more of the total surface area is affected, etc., so that the sum of these proportions is the total fraction of the body surface burned. Refinements may be made by observing temperature-time histories commensurate with pain, first-degree, second-, and third- degree burns if desired. We routinely note only "severely burned" (second-degree or worse) and "no burn" with appropriate comments when warranted (9).

In flame contact studies we have established as limits total envelopment in flames for a 3-second period; total envelopment to ensure a uniform

heat input, and 3 seconds as representative of the time for an uninjured man to run through 25-30 feet of flames, commensurate with the maximum exposure expected in a carrier deck crash exposure. Thus, the movement through the flames is set at a rate of about 10 ft/sec. The rate of movement is important, for convection currents which roll up the back surface are generated at this speed but not at significantly lower speeds. Burns are more severe in the back than in the front under these conditions and are so indicated in the manikin experiments.

It is also possible to determine the predicted severity of burns by continuous measurement of the temperature-time history before, during and after exposure and computation of total damage from the damage rate-time integral. However, the square-wave heat input for a fixed exposure time is a far easier approach because only the maximum surface temperature need be measured to determine the burn effect as illustrated in Table I.

Our present facility for such exposures is shown in Figure 16. Briefly it consists of a pit, 25 x 20 feet, in which aviation gasoline is spread on a water base and ignited to provide a flame path. A crane with a 20-foot boom rotates at a fixed rate of 4.8 rpm so that a manikin suspended from the boom is carried through the flames in 3 seconds. If need be, the exposure time may be varied between 2.5 and 3.3 seconds by suspending the manikin at different points between 17 and 22 feet from the center of rotation thus moving it through the flames at speeds from 8.5 to 10.5 ft/sec, respectively. A cinder block wall protects the crane operator during exposure, and the manikin before and after exposure. The entire facility is contained in a

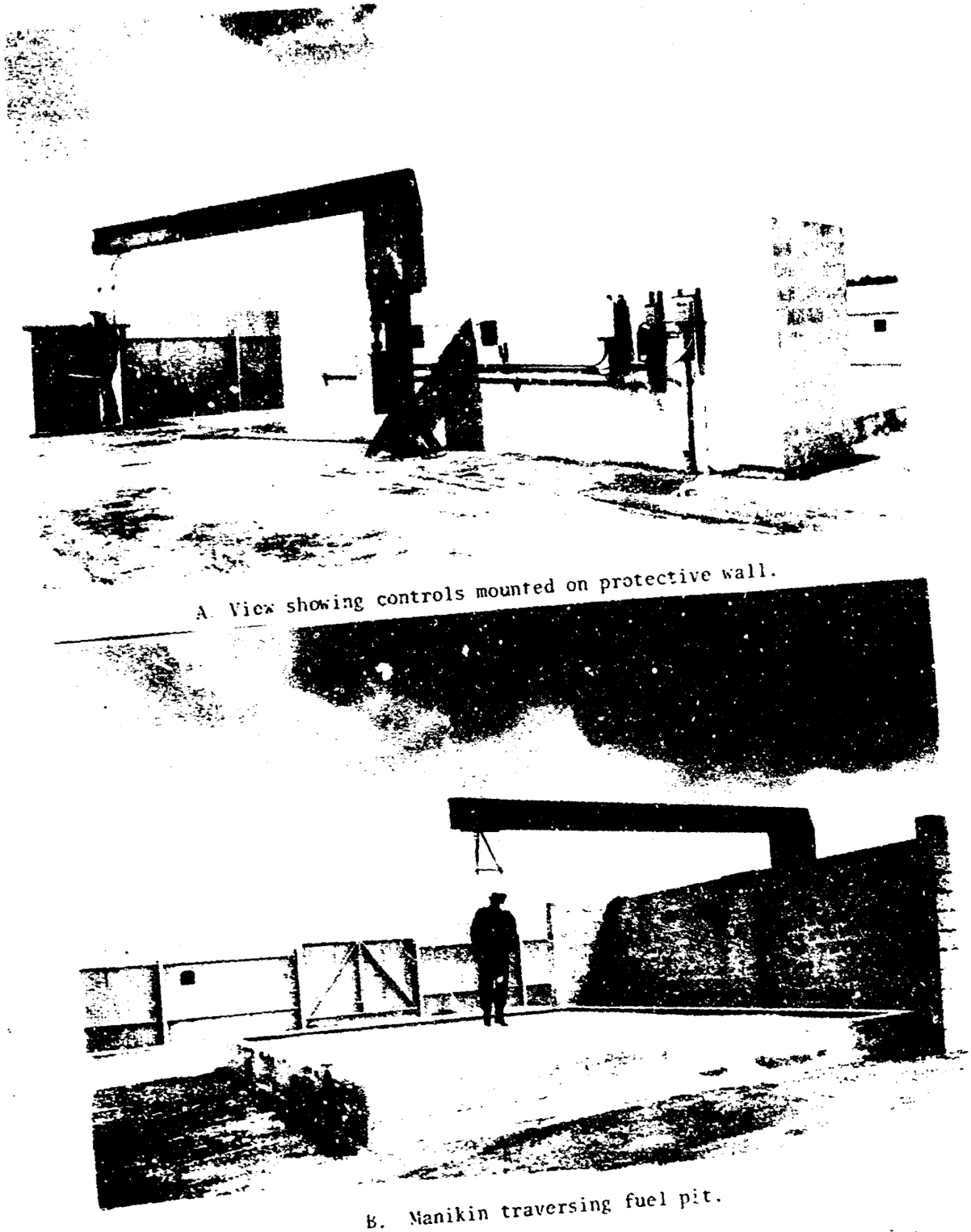

A. View showing controls mounted on protective wall.

B. Manikin traversing fuel pit.

Figure 16. Fuel flame facility for exposures in full-scale protection evaluations.

galvanized iron enclosure 8 feet high and provided wtih portholes for camera coverage and observation. At present protection from winds is adequate up to 10 mph gusts. Further modifications are in progress to improve this protection and to provide for more even distribution of the gasoline on the water base to prevent regional burn-outs during exposures. Routinely, calibrated paper detectors are used to measure the surface temperatures. Under development now is a thermocouple telemetry system for continuous measurement of these temperatures to provide for more flexibility in experimental procedures.

For evaluation of high-intensity thermal radiation protective clothing, heat is supplied by an arc of tungsten-in-quartz lamps arranged to conform to the shape of an aircraft cockpit canopy (Figure 17). Wind is blown over the canopy surface during exposures to eliminate hot air conduction effects. Irradiances and thermal loads are measured at the source, the outside surface of the canopy, and at various levels within the cockpit. Surface temperatures are measured on the manikin under the clothing and pain and burn assessments made as described before. Particulars demonstrating how predictions from small-scale laboratory evaluations were corroborated in the full-scale simulation are given in Stoll (10). In short, this study illustrates the effectiveness of absorbing radiation in a dark-colored outer layer and backing this layer with a low-conductivity material which slows the heat transfer to the skin beneath. In this way greater protection can be derived from a dark, absorptive assembly than from a white, reflective assembly which also has a high transmittance. Such considerations may

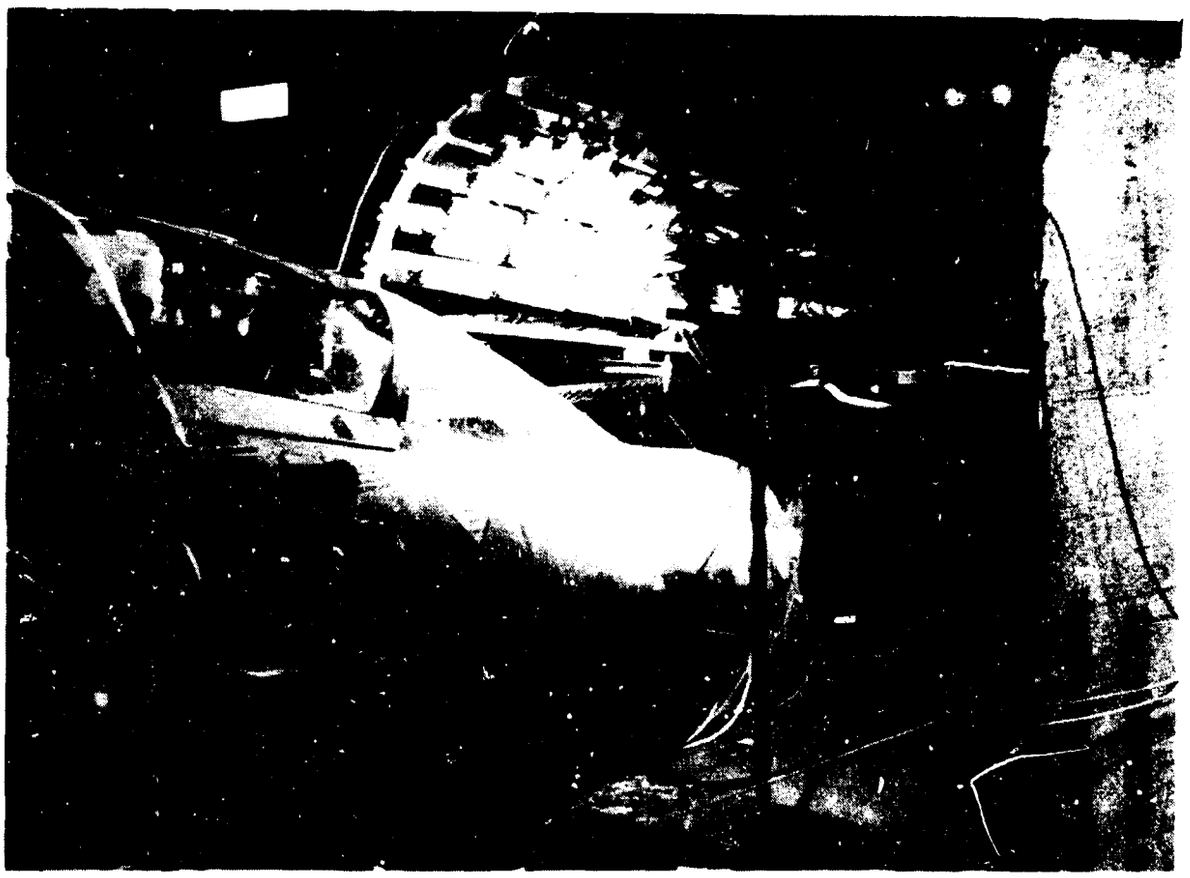

Figure 17. Quartz lamp heat source with F4 fuselage backed out from under arc.

be utilized to provide a variety of solutions to specific protection problems where the effects of optical and thermal properties and the modes of heat transfer are thoroughly understood.

REFERENCES

1. Stoll, A. M. and L. C. Greene, Relationship between Pain and Tissue Damage due to Thermal Radiation. J. Appl. Physiol. 14: 373-382, May 1959.
2. Moritz, A. R. and F. C. Henriques, Jr., Studies of Thermal Injury II: The relative importance of time and surface temperature in the causation of cutaneous burns. Am. J. Pathol. 23:695-719, Sept. 1947.
3. Stoll, A. M. A computer Method for the Determination of Tissue Damage Integrals from Experimental Data. IRE Trans. Med. Elect. ME7: 355-358, Oct. 1960.
4. Griffith, M. V. and G. K. Horton. The Transient Flow of Heat Through a Two-layer Wall. Proc. Phys. Soc. (London) 58:481, 1946.
5. Stoll, A. M., M. A. Chianta and L. R. Munroe, Flame Contact Studies, I, II, III, J. Heat Transfer, ASME Series C 449-456, August 1964.
6. Stoll, A. M. and M. A. Chianta, Burn Production and Prevention in Convective and Radiant Heat Transfer. Aerospace Med. 39: #10, 1097-1100, October 1968.
7. Stoll, A. M. and M. A. Chianta, A Method and Rating System for Evaluation of Thermal Protection. Aerospace Med. 40: #11, 1232-1238, November 1969.
8. Hardy, J. D. and G. F. Soderstrom, Heat Loss from the Nude Body and Peripheral Blood Flow at Temperatures of 22° to 35°C. J. Nutrition 16:493, 1938.
9. Stoll, A. M. Thermal Protection Capacity of Aviator's Textiles, Aerospace Med. 33:846-850, July 1962.

10. Stoll, A.M., M.A. Chianta, and L.B. Judge. Development of Practical High-Intensity Thermal Protection Systems. (In press) Presented at the 41st Annual Aerospace Medical Association Meeting, St. Louis, Missouri, April 1970.

UNCLASSIFIED
Security Classification

DOCUMENT CONTROL DATA - R & D

(Security classification of title, body of abstract and indexing annotation must be entered when the overall report is classified)

1. ORIGINATING ACTIVITY (Corporate author)
Aerospace Medical Research Department
Naval Air Development Center
Warminster, Pa. 18974

2a. REPORT SECURITY CLASSIFICATION
Unclassified

2b. GROUP

3. REPORT TITLE
Heat Transfer Through Fabrics

4. DESCRIPTIVE NOTES (Type of report and inclusive dates)
Interim Report

5. AUTHOR(S) (First name, middle initial, last name)
Alice M. Stoll
Maria A. Chianta

6. REPORT DATE
16 September 1970

7a. TOTAL NO. OF PAGES
33

7b. NO. OF REFS
10

8a. CONTRACT OR GRANT NO.

b. PROJECT NO.
AirTask A34531/202/70F32523401
Work Unit No. 2
AirTask A34531/202/70F12524402
Work Unit No. 7

9a. ORIGINATOR'S REPORT NUMBER(S)
NADC-MR-7017

9b. OTHER REPORT NO(S) (Any other numbers that may be assigned this report)

10. DISTRIBUTION STATEMENT
This report has been approved for public release and sale; its distribution is unlimited.

11. SUPPLEMENTARY NOTES

12. SPONSORING MILITARY ACTIVITY

13. ABSTRACT

Heat is transferred through fabrics by convection, conduction and radiation and under certain circumstances by vaporization. Each mode is subject to different physical principles but the effect of the total heat absorbed by underlying skin is the same: if the resultant skin temperature rise is sufficiently high and maintained sufficiently long, injury results. The extent of injury is predicted under certain controlled conditions and these conditions may be used to disclose protection principles appropriate to each mode of transfer.

DD FORM 1 NOV 65 1473 (PAGE 1)
S/N 0101-807-6801

UNCLASSIFIED
Security Classification

14 KEY WORDS	LINK A ROLE	LINK A WT	LINK B ROLE	LINK B WT	LINK C ROLE	LINK C WT
1. High-intensity thermal radiation protection						
2. Thermal radiation protective clothing						
3. Thermal protection						